



HAL
open science

Inhibitory modulation of the mitochondrial permeability transition by minocycline

Anne Gieseler, Adrian Tilman Schultze, Kathleen Kupsch, Mohammad Fahad Haroon, Gerald Wolf, Detlef Siemen, Peter Kreutzmann

► **To cite this version:**

Anne Gieseler, Adrian Tilman Schultze, Kathleen Kupsch, Mohammad Fahad Haroon, Gerald Wolf, et al.. Inhibitory modulation of the mitochondrial permeability transition by minocycline. *Biochemical Pharmacology*, 2009, 77 (5), pp.888. 10.1016/j.bcp.2008.11.003 . hal-00531839

HAL Id: hal-00531839

<https://hal.science/hal-00531839>

Submitted on 4 Nov 2010

HAL is a multi-disciplinary open access archive for the deposit and dissemination of scientific research documents, whether they are published or not. The documents may come from teaching and research institutions in France or abroad, or from public or private research centers.

L'archive ouverte pluridisciplinaire **HAL**, est destinée au dépôt et à la diffusion de documents scientifiques de niveau recherche, publiés ou non, émanant des établissements d'enseignement et de recherche français ou étrangers, des laboratoires publics ou privés.

Accepted Manuscript

Title: Inhibitory modulation of the mitochondrial permeability transition by minocycline

Authors: Anne Gieseler, Adrian Tilman Schultze, Kathleen Kupsch, Mohammad Fahad Haroon, Gerald Wolf, Detlef Siemen, Peter Kreutzmann



PII: S0006-2952(08)00788-0
DOI: doi:10.1016/j.bcp.2008.11.003
Reference: BCP 10003

To appear in: *BCP*

Received date: 30-9-2008
Revised date: 3-11-2008
Accepted date: 3-11-2008

Please cite this article as: Gieseler A, Schultze AT, Kupsch K, Haroon MF, Wolf G, Siemen D, Kreutzmann P, Inhibitory modulation of the mitochondrial permeability transition by minocycline, *Biochemical Pharmacology* (2008), doi:10.1016/j.bcp.2008.11.003

This is a PDF file of an unedited manuscript that has been accepted for publication. As a service to our customers we are providing this early version of the manuscript. The manuscript will undergo copyediting, typesetting, and review of the resulting proof before it is published in its final form. Please note that during the production process errors may be discovered which could affect the content, and all legal disclaimers that apply to the journal pertain.

Inhibitory modulation of the mitochondrial permeability transition by minocycline

Anne Gieseler ^{a,1}, Adrian Tilman Schultze ^{b,1}, Kathleen Kupsch ^a, Mohammad Fahad Haroon ^a, Gerald Wolf ^a, Detlef Siemen ^b, Peter Kreutzmann ^{a,*}

^a Institute of Medical Neurobiology, Otto-von-Guericke University Magdeburg, Leipziger Str. 44, D-39120 Magdeburg, Germany

^b Department of Neurology, Otto-von-Guericke University Magdeburg, Leipziger Str. 44, D-39120 Magdeburg, Germany

¹ These authors contributed equally to this work.

* Corresponding author:

Peter Kreutzmann, Ph.D.

Institute of Medical Neurobiology

Otto-von-Guericke University Magdeburg

Leipziger Str. 44

D-39120 Magdeburg

Germany

Phone: +49-(0)391-6714361

Fax: +49-(0)391-6714365

E-mail: peter.kreutzmann@med.ovgu.de

Abstract

1
2
3
4
5 The semisynthetic tetracycline derivative minocycline exerts neuroprotective
6
7 properties in various animal models of neurodegenerative disorders. Although anti-
8
9 inflammatory and anti-apoptotic effects are reported to contribute to the
10
11 neuroprotective action, the exact molecular mechanisms underlying the beneficial
12
13 properties of minocycline remain to be clarified. We analyzed the effects of
14
15 minocycline in a cell culture model of neuronal damage and in single-channel
16
17 measurements on isolated mitoplasts. Treatment of neuron-enriched cortical cultures
18
19 with rotenone, a high affinity inhibitor of the mitochondrial complex I, resulted in a
20
21 deregulation of the intracellular Ca^{2+} dynamics, as recorded by live cell imaging.
22
23 Minocycline (100 μM) and cyclosporin A (2 μM), a known inhibitor of the
24
25 mitochondrial permeability transition pore, decreased the rotenone-induced Ca^{2+}
26
27 deregulation by 60.9 % and 37.6 %, respectively. Investigations of the mitochondrial
28
29 permeability transition pore by patch-clamp techniques revealed for the first time a
30
31 dose-dependent reduction of the open probability by minocycline ($\text{IC}_{50} = 190 \text{ nM}$).
32
33 Additionally, we provide evidence for the high antioxidant potential of MC in our
34
35 model. In conclusion, the present data substantiate the beneficial properties of
36
37 minocycline as promising neuroprotectant by its inhibitory activity on the
38
39 mitochondrial permeability transition pore.
40
41
42
43
44
45
46
47
48
49
50
51
52
53
54
55
56
57
58
59
60
61
62
63
64
65

Keywords

Primary cortical neurons; Rotenone; Mitochondrial permeability transition;
Minocycline; Patch clamp

Abbreviations

CsA, cyclosporin A; DFF, 2',7'-difluorofluorescein; DIV, days *in vitro*; DMEM, Dulbecco's Modified Eagle Medium; DMSO, dimethylsulfoxide; DPPH, 2,2-diphenyl-1-picrylhydrazyl; Fluo-4 AM, fluo-4 pentaacetoxy-methylester; GFAP, glial fibrillary acid protein; HEPES, N-2-hydroxyethylpiperazine-N'-2-ethanesulfonic acid; MC, minocycline; mPTP, mitochondrial permeability transition pore; MTT, 3-[4,5-dimethylthiazol-2-yl]-2,5-diphenyl tetrazolium bromide; NMDA, N-methyl-D-aspartate; P_o , probability of being in the open state; PBS, phosphate-buffered saline; PD, Parkinson's disease; RLM, rat liver mitochondria; ROI, region of interest

1 Introduction

1
2
3 Minocycline (MC) is a semi-synthetic tetracycline derivative with proven and safe
4
5 clinical track record and mainly used in the treatment of acne vulgaris [1]. Originally
6
7 developed as an antibiotic with a broad-spectrum antibacterial activity, it shows
8
9 biological effects, which are fundamentally different from its antimicrobial action. An
10
11 increasing number of studies reported the potential use of MC as a cytoprotectant in
12
13 the treatment of several neurological disorders including amyotrophic lateral sclerosis
14
15 [2], multiple sclerosis [3], Alzheimer's disease [4], Huntington's disease [5], Leber's
16
17 hereditary optic neuropathy [6], and Parkinson's disease (PD) [7-9]. Furthermore,
18
19 neuroprotective potency of MC has been observed in experimental models of acute
20
21 cerebral ischemia [10, 11], spinal cord- [12-14] and traumatic brain injury [15]. But,
22
23 also contradictory and even detrimental effects of MC were reported recently [16-20],
24
25 pointing at the importance of a thorough understanding of the detailed cellular and
26
27 molecular mechanisms triggered by MC.
28
29

30
31 It has been suggested that the observed protection conferred by MC is based on its
32
33 anti-inflammatory and anti-oxidant properties, including the inhibition of matrix
34
35 metalloproteases [21], blockade of inducible nitric oxide synthase [22], as well as free
36
37 radical scavenging activity [23]. In addition, the MC-mediated neuroprotection is
38
39 associated with a blockade of caspases, inhibition of MAP kinase, and prevention of
40
41 cytochrome c release [2, 5, 14, 24]. But, a direct involvement of MC in mitochondrial
42
43 permeability transition is still a matter of debate [25].
44
45

46
47 Mitochondrial dysfunction is widely accepted to contribute to degeneration processes
48
49 in neurodegenerative diseases and neurotoxins impairing the oxidative
50
51 phosphorylation are used to create cellular and animal models for these disorders.
52
53

54
55 One environmental toxin used in PD-related models is rotenone [26], a natural
56
57
58
59
60
61
62
63
64
65

1 occurring complex keton. Due to its lipophilic character, rotenone crosses
2 membranes freely and accumulates in cytoplasm and mitochondria [27] where it
3
4 inhibits complex I of the mitochondrial respiratory chain by stopping the supply of
5
6 electrons to quinol (OH₂)-cytochrome c oxidoreductase [28]. This results in a dose-
7
8 dependent ATP-depletion, generation of free radicals, and finally apoptosis [29].
9
10 Although the rotenone model demonstrates potential relevance of the complex I
11
12 deficit in PD pathogenesis, the mechanisms through which dysfunction of complex I
13
14 might produce neurotoxicity are still unknown. It was reported that under pathological
15
16 conditions of low ATP, oxidative stress, and high cytosolic calcium concentration the
17
18 inner mitochondrial membrane permeability increases by formation of a large
19
20 nonselective pore, the mitochondrial permeability transition pore (mPTP). The
21
22 opening of this channel leads to an increase of the permeability to ions and small
23
24 solutes of less than 1.5 kDa, resulting in mitochondrial swelling, depolarization, and a
25
26 loss of membrane potential [30]. Concomitantly, the release of mitochondrial calcium
27
28 ions as well as pro-apoptotic factors (e.g. apoptosis-inducing factor, cytochrome c)
29
30 into the cytosol triggers signaling cascades leading to apoptosis and seems to cause
31
32 neuronal decline in neurodegenerative diseases [31].
33
34 Here we study the pro-apoptotic permeability transition triggered by rotenone-induced
35
36 complex I inhibition in cultivated cortical neurons with focus on the effect of MC-
37
38 application. Furthermore, we attempt to examine by single-channel measurements
39
40 whether MC affects directly the formation/activity of the mPTP.
41
42
43
44
45
46
47
48
49
50
51
52
53
54
55
56
57
58
59
60
61
62
63
64
65

2 Materials and methods

2.1 Chemicals

Cyclosporin A (CsA) and N-methyl-D-aspartate (NMDA) were obtained from Alexis (Lausen, Switzerland). If not especially mentioned, all other chemicals were purchased from Sigma (Steinheim, Germany). Stock solutions of rotenone (10 mM in DMSO) and MC (10 mM in appropriate water-based buffer) were prepared fresh daily. CsA (2 mM) was solubilized in 70 % (v/v) ethanol and stored at 4 °C.

2.2 Cell culture

All procedures for animal use were in strict accordance with the Animal Health and Care Committee of the State of Saxony-Anhalt, Germany. The animals (Wistar rats, Harlan-Winkelmann, Borcheln, Germany) were housed under controlled pathogen-free conditions with a cycle of 12 h light/12 h dark and food/water *ad libitum*. Rats were mated overnight and the following day was defined as embryonic day 1 (E1). Neuron-enriched cortical cultures were prepared from cerebral cortices of 16 days old rat embryos (E16). The cortices were removed, cleaned of meninges, and placed in Dulbecco's Modified Eagle Medium (DMEM; PAA Laboratories GmbH, Coelbe, Germany). After mechanical dispersion and centrifugation (5 min at 300 g), the dissociated cells were plated onto poly-D-lysine-coated (0.1 mg/ml in borate buffer, pH 8.4) 25 mm round glass coverslips placed in 35 mm culture dishes at a density of $1.5 \cdot 10^6$ cells/2 ml in DMEM medium with 2 % B-27 (serum-free supplement, Invitrogen, Karlsruhe, Germany). Cells were maintained 13 days *in vitro* (13. DIV) in a

1 humidified 5 % CO₂/ 95 % air atmosphere at 37 °C. Culture medium was replaced by
2 DMEM without B-27 supplement 24 h before use. Immunohistochemical
3
4 characterization of the cultures was performed using the primary SMI311-antibody
5 (1:1000; Convance, Berkely, USA) and GFAP-antibody (1:5000; Santa Cruz
6
7 Biotechnology, Santa Cruz, USA) to detect neurons and astrocytes, respectively.
8
9 Briefly, cells were fixed (4 % paraformaldehyde, 20 min) and incubated in blocking
10
11 solution (10 % donkey normal serum, 0.3 % Triton X-100, 0.1 % sodium azide) for
12
13 30 min followed by the application of the respective primary antibody (overnight at
14
15 4 °C). After washing with PBS containing 0.1 % Triton X-100 the cells were
16
17 sequentially incubated with the respective secondary antibody (1:1000, Cy2-
18
19 conjugated anti-mouse-IgG, Rockland, Gilbertsville, USA; Cy3-conjugated anti-goat-
20
21 IgG, Dianova, Hamburg, Germany) for 2-3 h, mounted, and examined on a confocal
22
23 fluorescence microscope (AXIOVERT 100M, LSM PASCAL, Zeiss, Jena, Germany).
24
25
26
27
28
29
30
31
32
33

34 **2.3 Cell viability assay**

35
36
37
38
39 Cell viability was assayed using MTT (3-(4,5-dimethylthiazol-2-yl)-2,5-
40
41 diphenyltetrazolium bromide), a yellow tetrazolium salt, which is reduced to purple
42
43 water-insoluble formazan by active cells. Cortical neurons were treated with different
44
45 concentrations of rotenone (100 pM, 500 pM, 1 nM, 5 nM, and 10 nM) for 24 h. The
46
47 medium was replaced by 1 ml PBS containing 1 mg MTT and incubated at 37 °C for
48
49 1 h. Afterwards, cells were permeabilized by DMSO and the extent of reduction of
50
51 MTT to formazan within the cells was measured spectrophotometrically (Lambda 2,
52
53 PerkinElmer, Norwalk, USA) at an absorbance of 570 nm.
54
55
56
57
58
59
60
61
62
63
64
65

2.4 Intracellular calcium measurements

1
2
3
4
5 Intracellular calcium concentrations were recorded by live cell imaging using cortical
6
7 cultures grown on glass coverslips for 13 DIV. After 45 min incubation with 2.5 μ M
8
9 fluo-4 pentaacetoxy-methylester (Fluo-4 AM; Invitrogen, Karlsruhe, Germany) the
10
11 coverslips were placed in a stainless steel chamber (Attofluor, 2 ml volume,
12
13 Molecular probes, Leiden, The Netherlands) and mounted on a thermostatically
14
15 controlled stage (37 °C) of an inverted confocal fluorescence microscope
16
17 (AXIOVERT 100M, LSM PASCAL, Zeiss, Jena, Germany). Cultures were superfused
18
19 (1 ml/min) with HEPES-buffer (140 mM NaCl, 5 mM KCl, 2 mM CaCl₂, 10 mM
20
21 glucose, and 10 mM HEPES, pH 7.47) for at least 2 min (baseline) followed by
22
23 subsequent stimulation with 200 μ M NMDA to induce an acute increase of cytosolic
24
25 Ca²⁺. Investigated drugs or vehicle (DMSO and Ethanol) were consistently applied
26
27 30 min before and during the Ca²⁺-measurements. Fluorescent images (excitation
28
29 488 nm and emission >505 nm) were captured sequentially (10 s intervals) and
30
31 experimental settings (including intensity of the laser, pinhole diameter, detector gain)
32
33 were kept uniform in all compared experiments. The fluorescence intensity data,
34
35 obtained as average intensity within regions of interest (ROIs over the somata of
36
37 about 10-25 individual cells), were quantified using the Zeiss LSM software. After
38
39 subtraction of a background noise the average of all analyzed cells of one
40
41 experiment (n=1) were used. The means of 5 time point values before a subsequent
42
43 addition of NMDA or at the end of the experiment were used for statistical analysis.
44
45
46 One way ANOVA followed by Dunnett T3 (SPSS Version 15.0.1.1) was performed to
47
48 asses the differences between the groups.
49
50
51
52
53
54
55
56
57
58
59
60
61
62
63
64
65

2.5 *Isolation of rat liver mitochondria, preparation of mitoplasts, and electrophysiology*

Rat liver mitochondria (RLM) were prepared as described previously [32] and the concentration of mitochondrial protein was determined by using the Biuret method. RLM were used for preparing mitoplasts i.e. fragile vesicles consisting of inner mitochondrial membrane after rupture of the outer membrane. They can be recognized by their absolutely round shape and one (in liver mitoplasts) dark spot. From mitoplasts single-channel currents were recorded by patch-clamp methods as explained in detail, previously [33]. Mitoplasts were obtained by hyposmotic shock: the ionic strength was lowered 10-fold by addition of a hypotonic medium (5 mM K-HEPES, 0.2 mM CaCl₂, pH 7.2). After one minute incubation at room temperature, isotonicity was restored by addition of hypertonic medium (750 mM KCl, 80 mM K-HEPES, 0.2 mM CaCl₂, pH 7.2).

For patch-clamp experiments borosilicate glass pipettes (Harvard Apparatus, Fircroft, Kent, UK) were polished to yield resistances of 10-15 MΩ. Free-floating mitoplasts were "chased" by means of an electrically driven micromanipulator and moved to their final position at the pipette tip by gentle suction. Gigaseals of 0.7-1.5 GΩ formed spontaneously in about 25 % of the trials, and currents were recorded by means of an EPC-7 amplifier (HEKA electronics, Lambrecht, Germany). Currents were low-pass filtered by a 4-pole Bessel filter at a corner frequency of 0.5 kHz. Data were recorded at a sample frequency of 4 kHz by means of the pClamp9.2 software (Axon instruments, Foster City, USA) which was also used for processing of the data. The measuring pipette was filled with HEPES-buffer (150 mM KCl, 0.3 mM CaCl₂, 20 mM K-HEPES, pH 7.2). Experiments were carried out at room temperature (25 ± 1 °C).

1
2
3
4
5
6
7
8
9
10
11
12
13
14
15
16
17
18
19
20
21
22
23
24
25
26
27
28
29
30
31
32
33
34
35
36
37
38
39
40
41
42
43
44
45
46
47
48
49
50
51
52
53
54
55
56
57
58
59
60
61
62
63
64
65

Test solutions were based on the HEPES-buffer and were applied through the glass capillaries of a peristaltic-pump driven flow system. Potentials are given as at the inner side of the membrane. Inward currents always deflect downward. The probability that the channel is in an open state (P_o) was determined by all-points analysis according to Loupatatzis *et al.* [34]. To the equation for fitting the dose-response curve by Michaelis-Menten kinetics, a term A was added accounting for a seemingly incomplete blockade of the mPTP in the early phase of the experiment. We collected the data in segments of one minute then dividing the mean of 6 segments in MC (skipping always the first) by the mean of 3 segments before MC as the normalized P_o . As development of the MC block took more than a minute, A accounts for the contribution of early records with incomplete blockade. Best fitting values were determined by means of the ENZFIT software.

2.6 ***Mitochondrial swelling and cytochrome c release from isolated mitochondria***

Swelling experiments on RLM (0.5 mg protein/ml) were performed in sucrose-based buffer (200 mM sucrose, 10 mM Tris, 1 mM KH_2PO_4 , 10 μM EGTA, 5 mM glutamate, and 5 mM malate, pH 7.2) and the decrease in light absorbance (620 nm) was recorded using a multiplate reader (Titertek Plus MS212, ICN, Frankfurt, Germany). RLM were pre-incubated with the investigated drugs or vehicle (ethanol) prior to stimulation with 100 μM Ca^{2+} . Afterwards, the release of cytochrome c into the buffer was determined by standard immunoblotting [6] using cytochrome c antibody (7H8.2C12, 1:500; BD Pharmingen, San Diego, USA).

2.7 *Intracellular oxidative stress assay*

The intracellular oxidative stress assay was performed according to the DFF-imaging procedure published previously [6]. Briefly, cortical cultures were incubated with 100 μM H₂DFF-DA (5-(and-6)-carboxy-2',7'-difluorodihydrofluorescein diacetate; Invitrogen, Karlsruhe, Germany) at 37 °C in a humidified 5 % CO₂ atmosphere for 60 min. The investigated drugs or vehicle (PBS) were applied 30 min prior to stimulation with 100 μM H₂O₂. The fluorescence intensity data, obtained as average intensity within ROIs over the somata of individual cells, were quantitatively analyzed using the Zeiss LSM software.

2.8 *DPPH radical scavenging assay*

The free-radical scavenging activity was determined by a procedure reported previously [35]. Briefly, DPPH (2,2-diphenyl-1-picrylhydrazyl; Fluka, Steinheim, Germany) was dissolved in 80 % methanol in water to a final concentration of 100 μM . The reactions were initiated by adding different concentrations of the tested drugs or of the vehicle (DMSO), incubated at 37 °C for 30 min. The absorbance was measured at 516 nm (Lambda 2, PerkinElmer, Norwalk, USA).

3 Results

3.1 Rotenone induces calcium deregulation in primary cortical neurons

In order to evaluate an adequate rotenone concentration that affected cortical neurons without inducing complete cell death, a colorimetric MTT-reduction assay was performed. Treatment with 100 pM, 500 pM, 1 nM, 5 nM, or 10 nM rotenone for 24 h resulted in a reduced formazan production of $89.0 \pm 6.3 \%$, $81.9 \pm 14.0 \%$, $72.3 \pm 9.5 \%$, $59.8 \pm 1.8 \%$, and $45.8 \pm 1.1 \%$, respectively, with statistical significance at concentrations of 5 and 10 nM ($p < 0.05$; Fig. 1A). The application of 10 nM rotenone for 24 h resulted in a cell survival of about 50 %. This concentration was used in the following experiments.

For evaluation of the involvement of the mitochondrial permeability transition pore (mPTP) in rotenone-mediated toxicity, changes of intracellular calcium were recorded in cortical neurons using the Ca^{2+} -imaging technique. The neuronal cultures from dissociated E16 rat cortices after 13 days *in vitro* (13 DIV) consist of a large population of neurons and single astroglia cells (Fig. 1B). Stimulation of these primary neurons with 200 μM NMDA for 2 min caused an increase of the Fluo-4 fluorescence immediately after the exposure. Within 5 min after NMDA stimulation, intensity returned to the basal level. The response of cell cultures after 13 DIV was stable and could be repeated by subsequent NMDA applications. This also indicates the viability of the cells during live cell imaging experiments (Fig. 2A). Treatment with 10 nM rotenone 30 min before and over the complete period of the experiment did not affect the amplitude of the Ca^{2+} -rise in cortical neurons. However, the fluorescence signal in the rotenone-treated groups did not return back to baseline levels after NMDA exposure as was the case in control cells (Fig. 2B). This Ca^{2+} -

1
2
3
4
5
6
7
8
9
10
11
12
13
14
15
16
17
18
19
20
21
22
23
24
25
26
27
28
29
30
31
32
33
34
35
36
37
38
39
40
41
42
43
44
45
46
47
48
49
50
51
52
53
54
55
56
57
58
59
60
61
62
63
64
65

deregulation became more obvious after repeated stimulations (2 to 3 times) with NMDA (Fig. 2C, D). In presence of both the mPTP inhibitor cyclosporin A (CsA, 2 μ M) and rotenone, the observed Ca^{2+} -deregulation was alleviated by 37.6 %. This indicates an involvement of mPTP-opening under these conditions (Fig. 2D).

3.2 *MC protects neurons against rotenone-induced Ca^{2+} -deregulation*

Simultaneous application of rotenone and 100 μ M MC decreased the rotenone-induced Ca^{2+} -deregulation. The analysis of the basal levels of cytosolic Ca^{2+} after the second stimulus did not show significant deviation after the application of MC (Fig. 2C). However, after MC treatment the final baseline of the Ca^{2+} -signal was significantly decreased by 60.9 % as compared with the rotenone-treated group after three NMDA stimuli (Fig. 2D). Thus, after repeated stimulations and transient rises of Ca^{2+} the presence of MC protected the cells from a Ca^{2+} -deregulation. Additionally, MC was more efficient than the mPTP inhibitor CsA at the tested concentration.

3.3 *Patch Clamp experiments reveal blocking of the mPTP by MC*

The most direct test for a possible blocking effect of MC on the mPTP is the single-channel experiment studying mitoplast membranes by patch-clamp techniques. The predominant channel of such patches showed a single-channel conductance of more than 1 nS, could be dose-dependently blocked by CsA, and was characterized by multiple substrates [34]. Patches demonstrating corresponding single-channel behavior were transferred to a pipe of the flow system that contained test solution with different concentrations of MC. Within 1-2 min the P_o declined to a lower level

1 (Fig. 3A) determined by all-points analysis as explained in methods. Inhibition was
2 concentration dependent and could be described by Michaelis-Menten kinetics with a
3
4 IC_{50} of 190 nM and a value A of 0.27 (Fig. 3B). In 4 out of 6 experiments with a
5
6 strong MC effect mPTP inhibition was partly reversible when switching to an isotonic
7
8 control solution. Thus, MC is able to inhibit the mPTP on the single-channel level.
9

10 11 12 13 14 15 **3.4 MC abolishes Ca^{2+} -induced swelling and cytochrome c release in isolated** 16 17 **RLM**

18
19
20
21
22 Investigations on isolated RLM proved, that MC (100 μ M) was able to inhibit swelling
23
24 induced by Ca^{2+} as measured by a reduced change of light absorbance (Fig. 4A).
25
26 Immunoblotting of the extra-mitochondrial fractions revealed that MC abolished the
27
28 Ca^{2+} -induced release of cytochrome c in RLM (Fig. 4B). Furthermore, MC triggered a
29
30 weak release of cytochrome c (without Ca^{2+}) under the tested conditions (Fig. 4B,
31
32 lane 1) which was comparable to the cytochrome c release observed after co-
33
34 treatment with Ca^{2+} (Fig. 4B, lane 5). In contrast to the data obtained by
35
36 immunoblotting, no swelling of MC-treated RLM (without Ca^{2+}) was observed (data
37
38 not shown).
39
40
41
42
43
44
45
46

47 48 **3.5 MC shows antioxidant activity inside the cells and is a powerful radical** 49 50 **scavenger**

51
52
53
54
55 Oxidative stress plays an important role in mitochondrial permeability transition [30,
56
57 36]. To examine a possible antioxidant capacity of MC in our cortical culture, cells
58
59 were preloaded with $H_2DFF-DA$ and the resulting DFF-fluorescence was measured.
60
61
62
63
64
65

1
2
3
4
5
6
7
8
9
10
11
12
13
14
15
16
17
18
19
20
21
22
23
24
25
26
27
28
29
30
31
32
33
34
35
36
37
38
39
40
41
42
43
44
45
46
47
48
49
50
51
52
53
54
55
56
57
58
59
60
61
62
63
64
65

The basal level of DFF fluorescence in untreated cells increased significantly after H₂O₂ (100 μM) exposure. Pre-treatment with 100 μM MC abolished the increase of the fluorescence signal (Fig. 5A), demonstrating the antioxidant activity of MC inside the cells.

In order to assess the general radical scavenging potency of MC, we used an assay that detected the reaction of the drug with DPPH, a stable artificial free radical. MC is an effective scavenger for DPPH as indicated by the concentration dependent decrease in light absorbance. The scavenging capacity is comparable with that of the well known radical scavenger L-ascorbic acid (Fig. 5B).

4 Discussion

1
2
3
4
5
6 It was our working hypothesis that treatment of cultivated cortical neurons with the
7 pesticide rotenone results in a disruption of the mitochondrial oxidative
8 phosphorylation chain by inhibition of complex I and hence elevation of reactive
9 oxygen species (ROS). Together with a high cytosolic calcium concentration, which
10 in turn induces formation and opening of the mitochondrial permeability transition
11 pore (mPTP), the release of pro-apoptotic factors is triggered. According to this “two-
12 hit” hypothesis [36], we established a cell culture model of neuronal damage in order
13 to test a possible inhibitory effect of the tetracycline derivative minocycline (MC) on
14 the induced mPTP-opening.
15
16
17
18
19
20
21
22
23
24
25
26

27 After chronic administration to rats rotenone reproduced some features of
28 Parkinson’s disease (PD) [26, 29] and also triggered degeneration in cultured PC-12
29 cells [37]. Based on these observations, and due to the well-defined chemical
30 property of rotenone as complex I inhibitor, we used this drug as inducer for neuronal
31 degeneration in our cell culture model. It turned out that cortical neurons of
32 embryonic rats cultivated for two weeks were highly sensitive to rotenone. This effect
33 was dose-dependent with a LD₅₀ of around 10 nM. The cells were affected in their
34 respiratory activity but without being committed to complete cell death. This result is
35 in contrast to other studies, in which 50-times higher concentrations of rotenone
36 (0.5 μM) were required for neuronal decline [38]. A possible explanation could be a
37 different cultivation method (application of the cytotoxic cytosine arabinoside) and the
38 lower age of the cultures in their study.
39
40
41
42
43
44
45
46
47
48
49
50
51
52
53
54
55

56 In our study, subsequent application of NMDA induced neuronal Ca²⁺-overload in the
57 cells. Under these conditions the Ca²⁺-equilibrium across the inner mitochondrial
58
59
60
61
62
63
64
65

1 membrane is shifted and mitochondria take up Ca^{2+} from the cytoplasm. This leads to
2 a stimulation of the respiratory chain and to an increase in ROS generation,
3
4 particularly in the presence of the complex I inhibitor rotenone. As a result, the mPTP
5 opens [39], the mitochondrial potential collapses, and Ca^{2+} is released into the
6
7 cytosol [40]. Such a Ca^{2+} -deregulation could be detected in rotenone-treated cells
8
9 during live cell calcium imaging. An involvement of the mPTP in the model is strongly
10
11 supported by the observed effect of the well-known mPTP inhibitor CsA, which
12
13 alleviated the Ca^{2+} -deregulation. This immune suppressive cyclic peptide binds to
14
15 cyclophilin D, a compound of the mPTP-complex, and prevents opening [41, 42].
16
17 However, the rotenone-mediated Ca^{2+} -deregulation is not entirely normalized by
18
19 CsA, indicating that other mechanisms are playing an additional role. In contrast to
20
21 CsA, the antibiotic MC was more effective to abolish the Ca^{2+} -deregulation mediated
22
23 by rotenone. This potential of MC to protect cells with defect complex I is in
24
25 accordance with a recent publication, wherein a malfunction of the respiratory chain
26
27 was initiated by point mutation of the mitochondrial DNA [6]. The ability of MC to
28
29 inhibit the formation of mPTP was also reported from groups focusing on isolated
30
31 brain and liver mitochondria [2, 43]. In contrast, Mansson *et al.* did not show a direct
32
33 inhibition of the mPTP in isolated brain mitochondria [25]. To clarify this issue, we
34
35 measured single-channel currents through the mPTP of mitoplasts. To our
36
37 knowledge, we show for the first time a blocking effect of MC on the mPTP by patch
38
39 clamp, indicating a direct interaction of MC with the mega pore. It must be noted,
40
41 however, that a mitoplast constitutes an artificial system in that the outer membrane
42
43 is missing and, secondly, the mitochondrial membrane potential is lost. Nevertheless,
44
45 mitoplasts have been proved to be useful tools to study successfully biophysical
46
47 questions and direct pharmacological interactions with the channel proteins in the
48
49 inner membrane [33, 34]. Additionally, it is remarkable that inhibition of the mPTP can
50
51
52
53
54
55
56
57
58
59
60
61
62
63
64
65

1
2
3
4
5
6
7
8
9
10
11
12
13
14
15
16
17
18
19
20
21
22
23
24
25
26
27
28
29
30
31
32
33
34
35
36
37
38
39
40
41
42
43
44
45
46
47
48
49
50
51
52
53
54
55
56
57
58
59
60
61
62
63
64
65

be observed at relatively high Ca^{2+} -concentrations. As calcium ions are known to activate the pore, the concentration of MC required for a full block are possibly even lower at lower Ca^{2+} -concentrations. The higher concentrations used here are necessary for establishing stable membrane patches at the tip of the measuring pipette.

The easier accessibility of the pore in mitoplasts for large modulating molecules as compared with intact mitochondria, the extremely sensitive measurement of the activity of single pores, and the high lipophilicity of MC [44] may be explanations for the observation that blockade of the mPTP required considerably lower MC concentrations in the patch-clamp experiments. Similarly, lower effective concentrations in mitoplast experiments than in experiments on intact mitochondria were reported before [33].

It has been considered that tetracyclines, including MC, can chelate Ca^{2+} . However, the presumable influence of MC on the extracellular Ca^{2+} concentration (e.g. in the intracellular calcium measurements) may be neglected because of the much higher concentration of Ca^{2+} in relation to MC in the buffer used.

Our data confirm earlier reports about the ability of MC to inhibit Ca^{2+} -induced swelling of rat liver mitochondria [43]. Additionally, the observed decrease of Ca^{2+} -triggered release of cytochrome c in the presence of MC supports previously reported protective effects of MC on the mPTP. A remarkable result was the finding that MC per se induced a weak release of cytochrome c without any detectable mitochondrial swelling. This observation may perhaps be an explanation for the observed detrimental effects of MC [16, 18-20] and requires further clarification.

Due to the fact that the observed changes of the intracellular Ca^{2+} -dynamics caused by rotenone could not be abolished completely by the mPTP-inhibitor CsA other mechanisms than mPTP-opening may play a role. The higher potential of MC, as

1 compared to CsA, to normalize the rotenone-triggered Ca^{2+} -deregulation may be
2 explained by the antioxidant properties of MC. This was also proved in our
3
4 experiments on cortical neurons after H_2O_2 -induction. Using a cell-free assay of
5
6 antioxidant-potency, our obtained data confirm additionally that MC is a direct
7
8 antioxidant [23] with a comparable potential as L-ascorbic acid.
9

10
11 In conclusion, rotenone-induced Ca^{2+} -deregulation of cultivated cortical neurons is
12
13 mediated by mitochondrial permeability transition. The promising cytoprotectant MC
14
15 is able to counteract this process. We show here a direct inhibitory interaction of MC
16
17 with the mPTP and confirm the high antioxidant potential of this multifaceted
18
19 tetracycline derivative. These findings point out the potential of MC for the treatment
20
21 of disorders related to oxidative stress and/or increased mPTP-opening in general. It
22
23 must be noted, however, that there are clear indications for additional detrimental
24
25 effects of MC, which makes the clinical application of MC rather doubtful [20].
26
27
28
29
30
31 Therefore, further investigations needed for clarification of the negative action of MC.
32
33
34
35
36
37
38
39
40
41
42
43
44
45
46
47
48
49
50
51
52
53
54
55
56
57
58
59
60
61
62
63
64
65

References

- 1
2
3
4
5 1. Goulden V, Glass D, Cunliffe WJ, Safety of long-term high-dose minocycline in
6
7 the treatment of acne. *Br J Dermatol.* **134**(4): 693-5., 1996.
- 8
9
10 2. Zhu S, Stavrovskaya IG, Drozda M, Kim BY, Ona V, Li M, et al., Minocycline
11
12 inhibits cytochrome c release and delays progression of amyotrophic lateral
13
14 sclerosis in mice. *Nature* **417**(6884): 74-8, 2002.
- 15
16
17 3. Brundula V, Rewcastle NB, Metz LM, Bernard CC, Yong VW, Targeting
18
19 leukocyte MMPs and transmigration: minocycline as a potential therapy for
20
21 multiple sclerosis. *Brain* **125**(Pt 6): 1297-308, 2002.
- 22
23
24 4. Choi Y, Kim HS, Shin KY, Kim EM, Kim M, Park CH, et al., Minocycline
25
26 attenuates neuronal cell death and improves cognitive impairment in Alzheimer's
27
28 disease models. *Neuropsychopharmacology* **32**(11): 2393-404, 2007.
- 29
30
31 5. Chen M, Ona VO, Li M, Ferrante RJ, Fink KB, Zhu S, et al., Minocycline inhibits
32
33 caspase-1 and caspase-3 expression and delays mortality in a transgenic mouse
34
35 model of Huntington disease. *Nat Med* **6**(7): 797-801, 2000.
- 36
37
38 6. Haroon MF, Fatima A, Scholer S, Gieseler A, Horn TF, Kirches E, et al.,
39
40 Minocycline, a possible neuroprotective agent in Leber's hereditary optic
41
42 neuropathy (LHON): Studies of cybrid cells bearing 11778 mutation. *Neurobiol*
43
44 *Dis* **28**: 237-250, 2007.
- 45
46
47 7. Du Y, Ma Z, Lin S, Dodel RC, Gao F, Bales KR, et al., Minocycline prevents
48
49 nigrostriatal dopaminergic neurodegeneration in the MPTP model of Parkinson's
50
51 disease. *Proc Natl Acad Sci U S A* **98**(25): 14669-74, 2001.
- 52
53
54 8. He Y, Appel S, Le W, Minocycline inhibits microglial activation and protects nigral
55
56 cells after 6-hydroxydopamine injection into mouse striatum. *Brain Res* **909**(1-2):
57
58 187-93, 2001.
- 59
60
61
62
63
64
65

- 1
2
3
4
5
6
7
8
9
10
11
12
13
14
15
16
17
18
19
20
21
22
23
24
25
26
27
28
29
30
31
32
33
34
35
36
37
38
39
40
41
42
43
44
45
46
47
48
49
50
51
52
53
54
55
56
57
58
59
60
61
62
63
64
65
9. Wu DC, Jackson-Lewis V, Vila M, Tieu K, Teismann P, Vadseth C, et al., Blockade of microglial activation is neuroprotective in the 1-methyl-4-phenyl-1,2,3,6-tetrahydropyridine mouse model of Parkinson disease. *J Neurosci* **22**(5): 1763-71, 2002.
 10. Yrjanheikki J, Keinanen R, Pellikka M, Hokfelt T, Koistinaho J, Tetracyclines inhibit microglial activation and are neuroprotective in global brain ischemia. *Proc Natl Acad Sci U S A* **95**(26): 15769-74, 1998.
 11. Yrjanheikki J, Tikka T, Keinanen R, Goldsteins G, Chan PH, Koistinaho J, A tetracycline derivative, minocycline, reduces inflammation and protects against focal cerebral ischemia with a wide therapeutic window. *Proc Natl Acad Sci U S A* **96**(23): 13496-500, 1999.
 12. Stirling DP, Khodarahmi K, Liu J, McPhail LT, McBride CB, Steeves JD, et al., Minocycline treatment reduces delayed oligodendrocyte death, attenuates axonal dieback, and improves functional outcome after spinal cord injury. *J Neurosci* **24**(9): 2182-90, 2004.
 13. Wells JE, Hurlbert RJ, Fehlings MG, Yong VW, Neuroprotection by minocycline facilitates significant recovery from spinal cord injury in mice. *Brain* **126**(Pt 7): 1628-37, 2003.
 14. Teng YD, Choi H, Onario RC, Zhu S, Desilets FC, Lan S, et al., Minocycline inhibits contusion-triggered mitochondrial cytochrome c release and mitigates functional deficits after spinal cord injury. *Proc Natl Acad Sci U S A* **101**(9): 3071-6, 2004.
 15. Sanchez Mejia RO, Ona VO, Li M, Friedlander RM, Minocycline reduces traumatic brain injury-mediated caspase-1 activation, tissue damage, and neurological dysfunction. *Neurosurgery* **48**(6): 1393-9; discussion 1399-401, 2001.

- 1
2
3
4
5
6
7
8
9
10
11
12
13
14
15
16
17
18
19
20
21
22
23
24
25
26
27
28
29
30
31
32
33
34
35
36
37
38
39
40
41
42
43
44
45
46
47
48
49
50
51
52
53
54
55
56
57
58
59
60
61
62
63
64
65
16. Cornet S, Spinnewyn B, Delaflotte S, Charnet C, Roubert V, Favre C, et al., Lack of evidence of direct mitochondrial involvement in the neuroprotective effect of minocycline. *Eur J Pharmacol* **505**(1-3): 111-9, 2004.
 17. Diguët E, Gross CE, Tison F, Bezard E, Rise and fall of minocycline in neuroprotection: need to promote publication of negative results. *Exp Neurol* **189**(1): 1-4, 2004.
 18. Fernandez-Gomez FJ, Gomez-Lazaro M, Pastor D, Calvo S, Aguirre N, Galindo MF, et al., Minocycline fails to protect cerebellar granular cell cultures against malonate-induced cell death. *Neurobiol Dis* **20**(2): 384-91, 2005.
 19. Keilhoff G, Langnaese K, Wolf G, Fansa H, Inhibiting effect of minocycline on the regeneration of peripheral nerves. *Dev Neurobiol* **67**(10): 1382-95., 2007.
 20. Gordon PH, Moore DH, Miller RG, Florence JM, Verheijde JL, Doorish C, et al., Efficacy of minocycline in patients with amyotrophic lateral sclerosis: a phase III randomised trial. *Lancet Neurol.* **6**(12): 1045-53, 2007.
 21. Golub LM, Lee HM, Ryan ME, Giannobile WV, Payne J, Sorsa T, Tetracyclines inhibit connective tissue breakdown by multiple non-antimicrobial mechanisms. *Adv Dent Res* **12**(2): 12-26, 1998.
 22. Amin AR, Attur MG, Thakker GD, Patel PD, Vyas PR, Patel RN, et al., A novel mechanism of action of tetracyclines: effects on nitric oxide synthases. *Proc Natl Acad Sci U S A* **93**(24): 14014-9, 1996.
 23. Kraus RL, Pasieczny R, Lariosa-Willingham K, Turner MS, Jiang A, Trauger JW, Antioxidant properties of minocycline: neuroprotection in an oxidative stress assay and direct radical-scavenging activity. *Journal of Neurochemistry* **94**(3): 819-27, 2005.
 24. Wang X, Zhu S, Drozda M, Zhang W, Stavrovskaya IG, Cattaneo E, et al., Minocycline inhibits caspase-independent and -dependent mitochondrial cell

- 1 death pathways in models of Huntington's disease. *Proc Natl Acad Sci U S A*
2 **100**(18): 10483-7, 2003.
3
4
5 25. Mansson R, Hansson MJ, Morota S, Uchino H, Ekdahl CT, Elmer E, Re-
6 evaluation of mitochondrial permeability transition as a primary neuroprotective
7 target of minocycline. *Neurobiol Dis* **25**(1): 198-205, 2007.
8
9
10
11 26. Betarbet R, Sherer TB, MacKenzie G, Garcia-Osuna M, Panov AV, Greenamyre
12 JT, Chronic systemic pesticide exposure reproduces features of Parkinson's
13 disease. *Nat Neurosci* **3**(12): 1301-6, 2000.
14
15
16
17 27. Talpade DJ, Greene JG, Higgins DS, Jr., Greenamyre JT, In vivo labeling of
18 mitochondrial complex I (NADH:ubiquinone oxidoreductase) in rat brain using
19 [(3)H]dihydrorotenone. *J Neurochem* **75**(6): 2611-21, 2000.
20
21
22
23 28. Degli Esposti M, Inhibitors of NADH-ubiquinone reductase: an overview. *Biochim*
24 *Biophys Acta* **1364**(2): 222-35, 1998.
25
26
27
28 29. Sherer TB, Betarbet R, Testa CM, Seo BB, Richardson JR, Kim JH, et al.,
29 Mechanism of toxicity in rotenone models of Parkinson's disease. *J Neurosci*
30 **23**(34): 10756-64, 2003.
31
32
33
34 30. Crompton M, The mitochondrial permeability transition pore and its role in cell
35 death. *Biochem J* **341** (Pt 2): 233-49, 1999.
36
37
38
39 31. Halestrap AP, Calcium, mitochondria and reperfusion injury: a pore way to die.
40 *Biochem Soc Trans* **34**(Pt 2): 232-7, 2006.
41
42
43
44 32. Kupsch K, Parvez S, Siemen D, Wolf G, Modulation of the permeability transition
45 pore by inhibition of the mitochondrial K(ATP) channel in liver vs. brain
46 mitochondria. *J Membr Biol* **215**(2-3): 69-74., 2007.
47
48
49
50 33. Sayeed I, Parvez S, Winkler-Stuck K, Seitz G, Trieu I, Wallesch CW, et al., Patch
51 clamp reveals powerful blockade of the mitochondrial permeability transition pore
52 by the D2-receptor agonist pramipexole. *Faseb J* **20**(3): 556-8, 2006.
53
54
55
56
57
58
59
60
61
62
63
64
65

- 1
2
3
4
5
6
7
8
9
10
11
12
13
14
15
16
17
18
19
20
21
22
23
24
25
26
27
28
29
30
31
32
33
34
35
36
37
38
39
40
41
42
43
44
45
46
47
48
49
50
51
52
53
54
55
56
57
58
59
60
61
62
63
64
65
34. Loupatatzis C, Seitz G, Schonfeld P, Lang F, Siemen D, Single-channel currents of the permeability transition pore from the inner mitochondrial membrane of rat liver and of a human hepatoma cell line. *Cell Physiol Biochem* **12**(5-6): 269-78, 2002.
 35. Lorenz P, Roychowdhury S, Engelmann M, Wolf G, Horn TF, Oxyresveratrol and resveratrol are potent antioxidants and free radical scavengers: effect on nitrosative and oxidative stress derived from microglial cells. *Nitric Oxide* **9**(2): 64-76, 2003.
 36. Brookes PS, Yoon Y, Robotham JL, Anders MW, Sheu SS, Calcium, ATP, and ROS: a mitochondrial love-hate triangle. *Am J Physiol Cell Physiol* **287**(4): C817-33, 2004.
 37. Hartley A, Stone JM, Heron C, Cooper JM, Schapira AH, Complex I inhibitors induce dose-dependent apoptosis in PC12 cells: relevance to Parkinson's disease. *J Neurochem* **63**(5): 1987-90, 1994.
 38. Pei W, Liou AK, Chen J, Two caspase-mediated apoptotic pathways induced by rotenone toxicity in cortical neuronal cells. *Faseb J* **17**(3): 520-2, 2003.
 39. Takeyama N, Matsuo N, Tanaka T, Oxidative damage to mitochondria is mediated by the Ca(2+)-dependent inner-membrane permeability transition. *Biochem J* **294** (Pt 3): 719-25, 1993.
 40. Dahlem YA, Wolf G, Siemen D, Horn TF, Combined modulation of the mitochondrial ATP-dependent potassium channel and the permeability transition pore causes prolongation of the biphasic calcium dynamics. *Cell Calcium* **39**(5): 387-400, 2006.
 41. Halestrap AP, Connern CP, Griffiths EJ, Kerr PM, Cyclosporin A binding to mitochondrial cyclophilin inhibits the permeability transition pore and protects

1 hearts from ischaemia/reperfusion injury. *Mol Cell Biochem* **174**(1-2): 167-72,
2 1997.

3
4 42. Zoratti M, Szabo I, De Marchi U, Mitochondrial permeability transitions: how
5 many doors to the house? *Biochim Biophys Acta* **1706**(1-2): 40-52, 2005.

6
7 43. Fernandez-Gomez FJ, Galindo MF, Gomez-Lazaro M, Gonzalez-Garcia C, Cena
8 V, Aguirre N, et al., Involvement of mitochondrial potential and calcium buffering
9 capacity in minocycline cytoprotective actions. *Neuroscience* **133**(4): 959-67,
10 2005.

11
12 44. Allen JC, Minocycline. *Ann Intern Med* **85**(4): 482-7, 1976.
13
14
15
16
17
18
19
20
21
22
23
24
25

26 **Acknowledgements**

27
28
29
30
31 The support and helpful discussions of Dr S. Kropf (Institute of Biometry and Medical
32 Informatics, Magdeburg) and Dr P. Schönfeld (Institute of Biochemistry, Magdeburg)
33 are gratefully appreciated. We thank H. Baumann and H. Goldammer for their expert
34 technical assistance. This work was supported by grants from the German Federal
35 Ministry of Education and Research (BMBF 01ZZ0407).
36
37
38
39
40
41
42
43
44
45
46
47
48
49
50
51
52
53
54
55
56
57
58
59
60
61
62
63
64
65

Figure legends:**Fig. 1.**

Rotenone decreases cell viability of primary cortical cell cultures. (A) Primary cortical cultures were treated for 24 h with different concentrations of rotenone. Cell viability was detected via MTT-reduction (see materials and methods). Data in percent of controls shown as means \pm S.E.M. (n=3). Statistical significance between rotenone-treated and untreated cells are indicated (* p<0.05, ** p<0.01).

(B) Immunohistochemical analysis of the primary cortical cell culture by using the neurofilament marker SMI311 (green) and GFAP (red) demonstrate the existence of neurons at 13 DIV (bar 20 μ m, representative image).

Fig. 2.

Stimulation of primary cortical cell cultures with NMDA (200 μ M, 3 times) leads to an elevated Ca^{2+} -concentration that was reversed during wash-out. (A) Imaging of intracellular Ca^{2+} -dynamics without drug (Vehicle, triangle), after application of 10 nM rotenone alone (black) and in combination with 2 μ M CsA (grey cross) or 100 μ M MC (grey circle). Presented are means (n=5) of Fluo-4 fluorescence intensities normalized to the highest signal (100 %). Statistical analysis of the intracellular Ca^{2+} -signals after the first (B), after the second (C), and after the third stimulus of NMDA (D). Data are shown as normalized means \pm S.E.M. (n=5). Acute treatment of 10 nM rotenone led to a calcium deregulation in primary cortical neurons. Simultaneous application of the mPTP-inhibitor CsA partially protected neurons from a rotenone-induced calcium deregulation, indicating involvement of the mPTP. In presence of MC this effect was more pronounced.

Fig. 3.

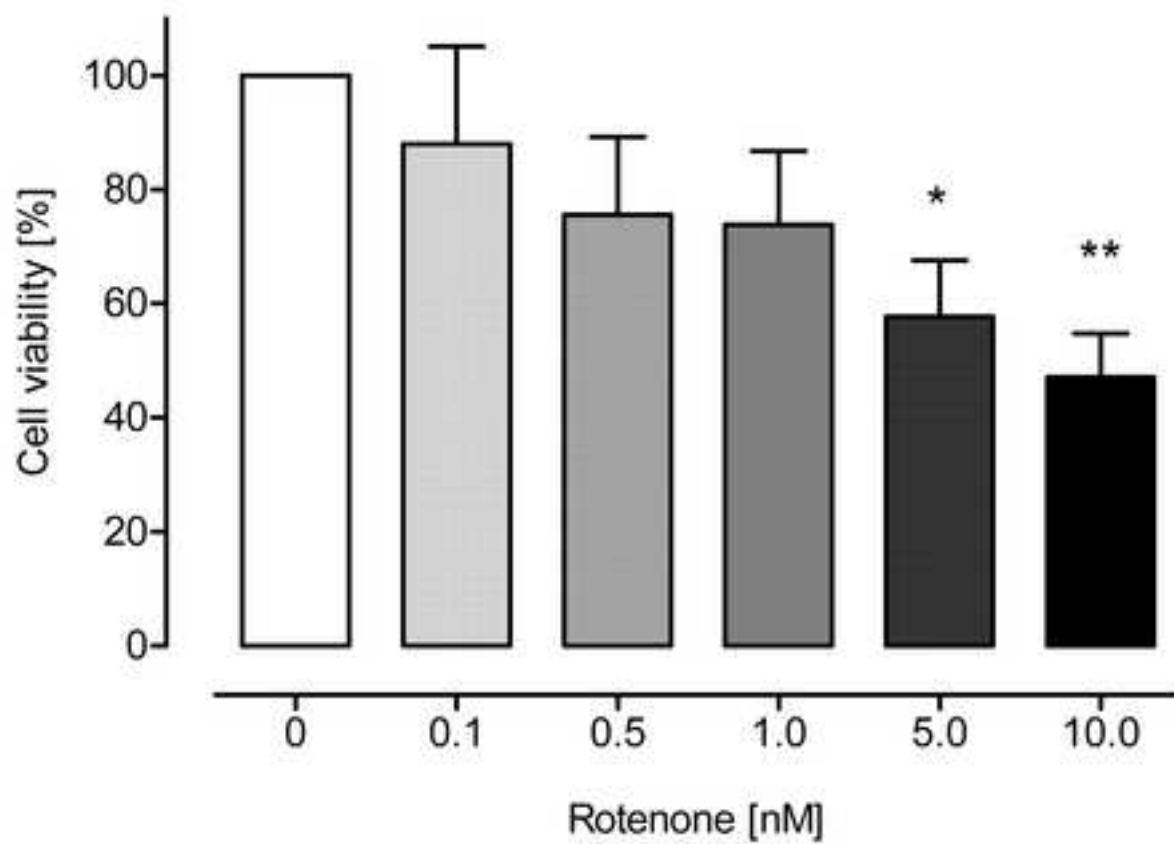
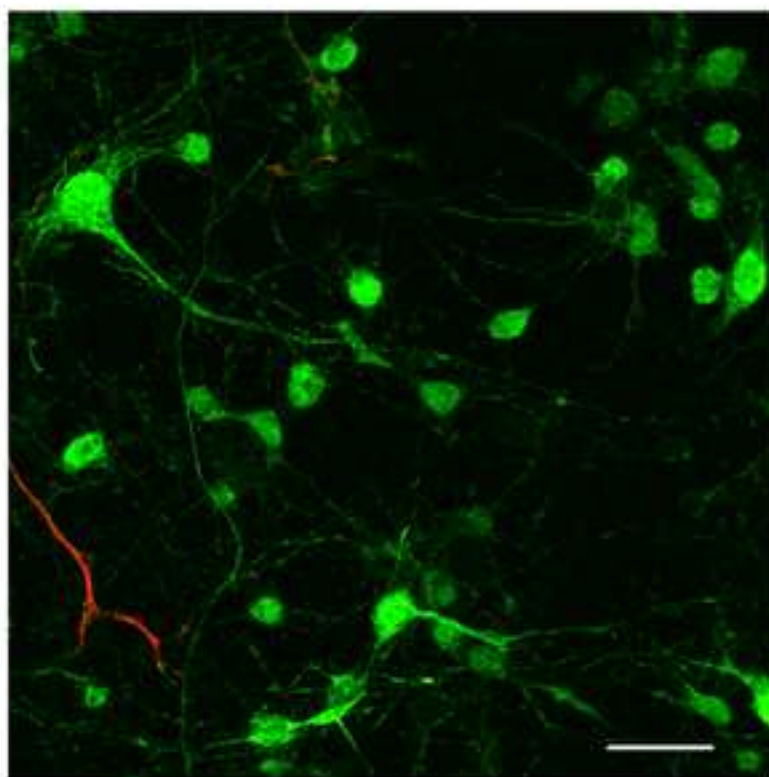
1
2 MC inhibits the mPTP of liver mitoplasts. (A) Single channel records from a mitoplast
3
4 before, 403 s after switching to a high (10 μM) MC concentration, and 317 s after
5
6 returning to an isotonic control solution. Dashed lines and arrows are giving the
7
8 closed state of the mPTP. MC reduced the open probability and the effect is
9
10 irreversible at this relatively high concentration. (B) The blocking effect of MC on the
11
12 mPTP of liver mitoplasts is dose dependent. Dose-response relation measured at 5
13
14 different concentrations of MC by single-channel experiments. The measuring points
15
16 give the normalized P_o (\pm S.E.M.) determined by all-point analysis and were fitted
17
18 best by Michaelis-Menten kinetics (continuous curve) with a IC_{50} of 190 nM and a
19
20 factor $A = 0.27$ (for significance of A see methods). The point used as the normalized
21
22 zero-concentration was taken from the mean of the P_o of the 3 min preceding
23
24 application of MC for each of 7 experiments.
25
26
27
28
29
30
31
32
33

Fig. 4.

34
35 MC inhibits Ca^{2+} -induced swelling and it modulates the release of cytochrome c in
36
37 RLM. (A) Swelling was measured in sucrose-based buffer as decrease in light
38
39 absorbance induced by 100 μM Ca^{2+} . After establishing a baseline the investigated
40
41 drugs were applied (black arrow). Pre-incubation with CsA (1 μM) completely
42
43 inhibited the Ca^{2+} -induced swelling, while in 100 μM MC-treated samples a transient
44
45 mild shrinkage was observed immediately after addition of Ca^{2+} . Data are presented
46
47 as means \pm S.E.M. ($n = 3$). (B) Immunoblotting demonstrated a strong release of
48
49 cytochrome c of RLM into the medium by Ca^{2+} , which was reduced by MC or was
50
51 completely blocked by CsA. MC (100 μM) alone showed a similar release of
52
53 cytochrome c as it did in combination with Ca^{2+} . A control without Ca^{2+} and without
54
55 MC did not show any cytochrome c release.
56
57
58
59
60
61
62
63
64
65

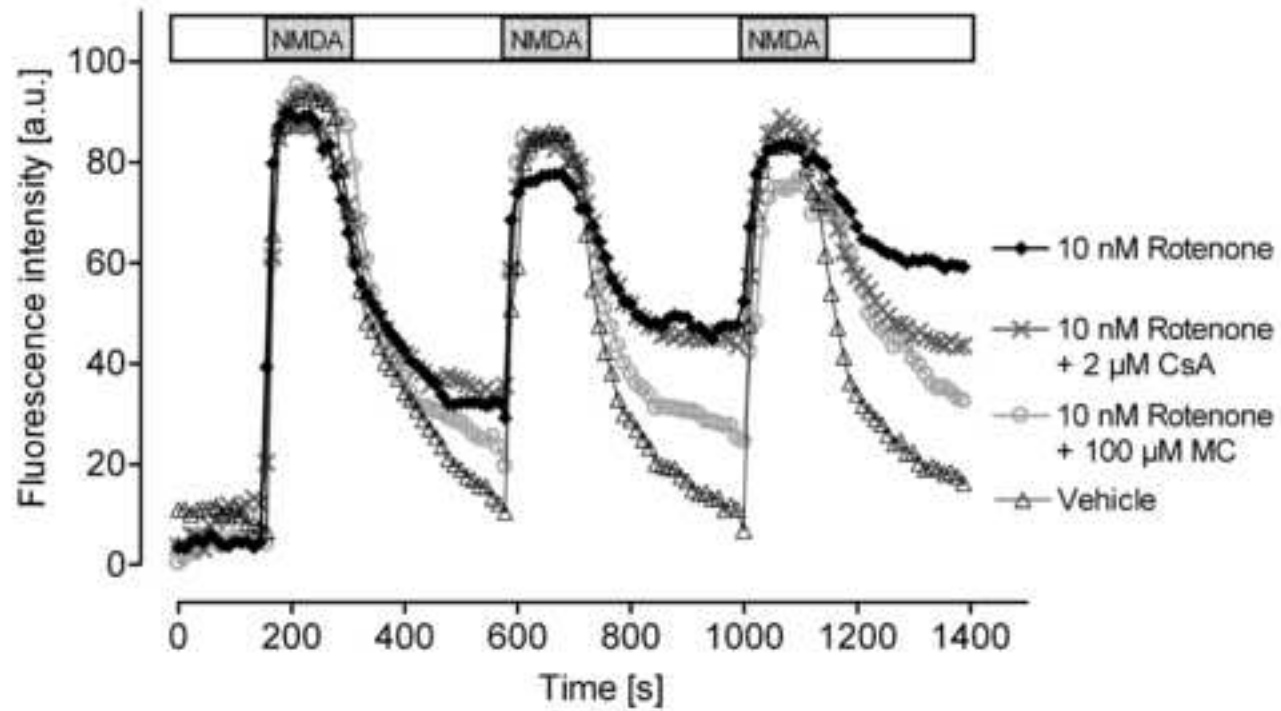
Fig. 5.

MC is a powerful free radical scavenger. (A) Fluorimetric analysis of oxidative stress induced by application of 100 μM H_2O_2 in primary cortical cultures (13 DIV). $\text{H}_2\text{DFF-DA}$ preloaded cells (100 μM , 1 h) showed a strong increase in DFF-fluorescence upon exposure to H_2O_2 . Pre-treatment with MC (100 μM) almost abolished the increase of the fluorescence signal. (B) MC scavenged the model radical DPPH at a comparable rate as did L-ascorbic acid. DPPH spectrophotometric assay is based on the quenching effect of radical scavengers on the absorbance of DPPH.

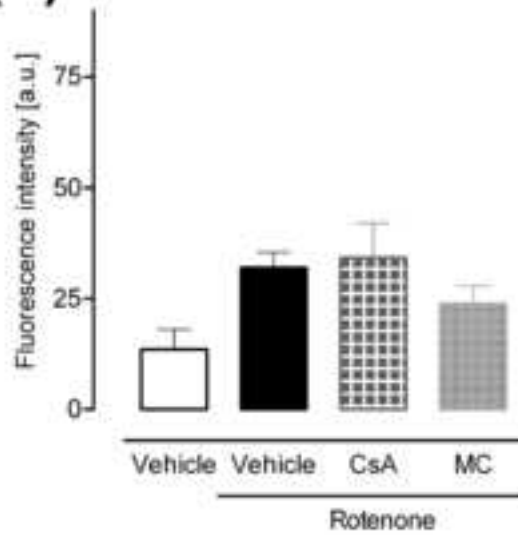
(A)**(B)**



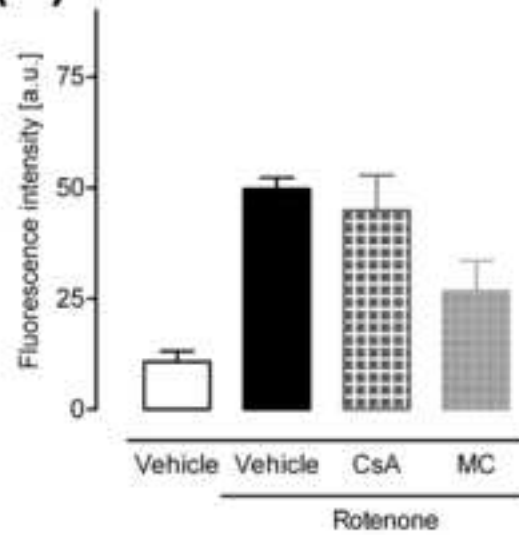
(A)



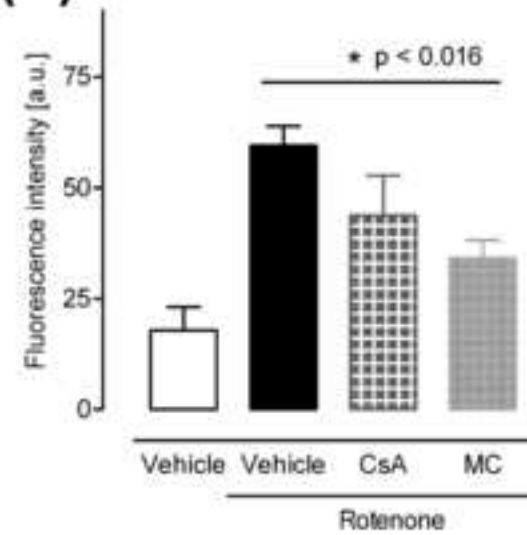
(B)



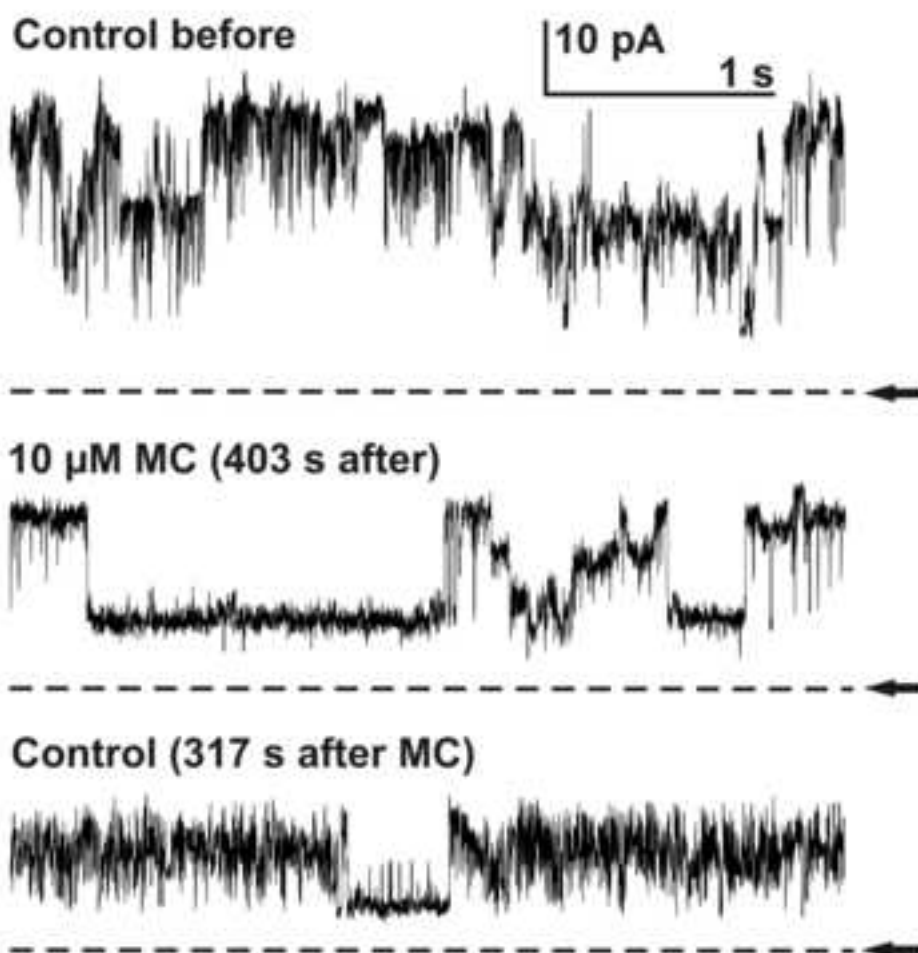
(C)



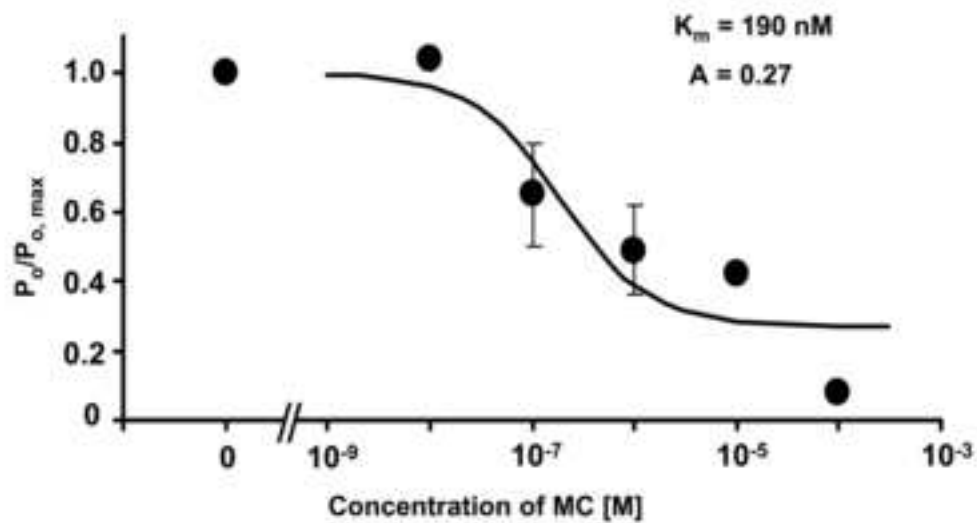
(D)

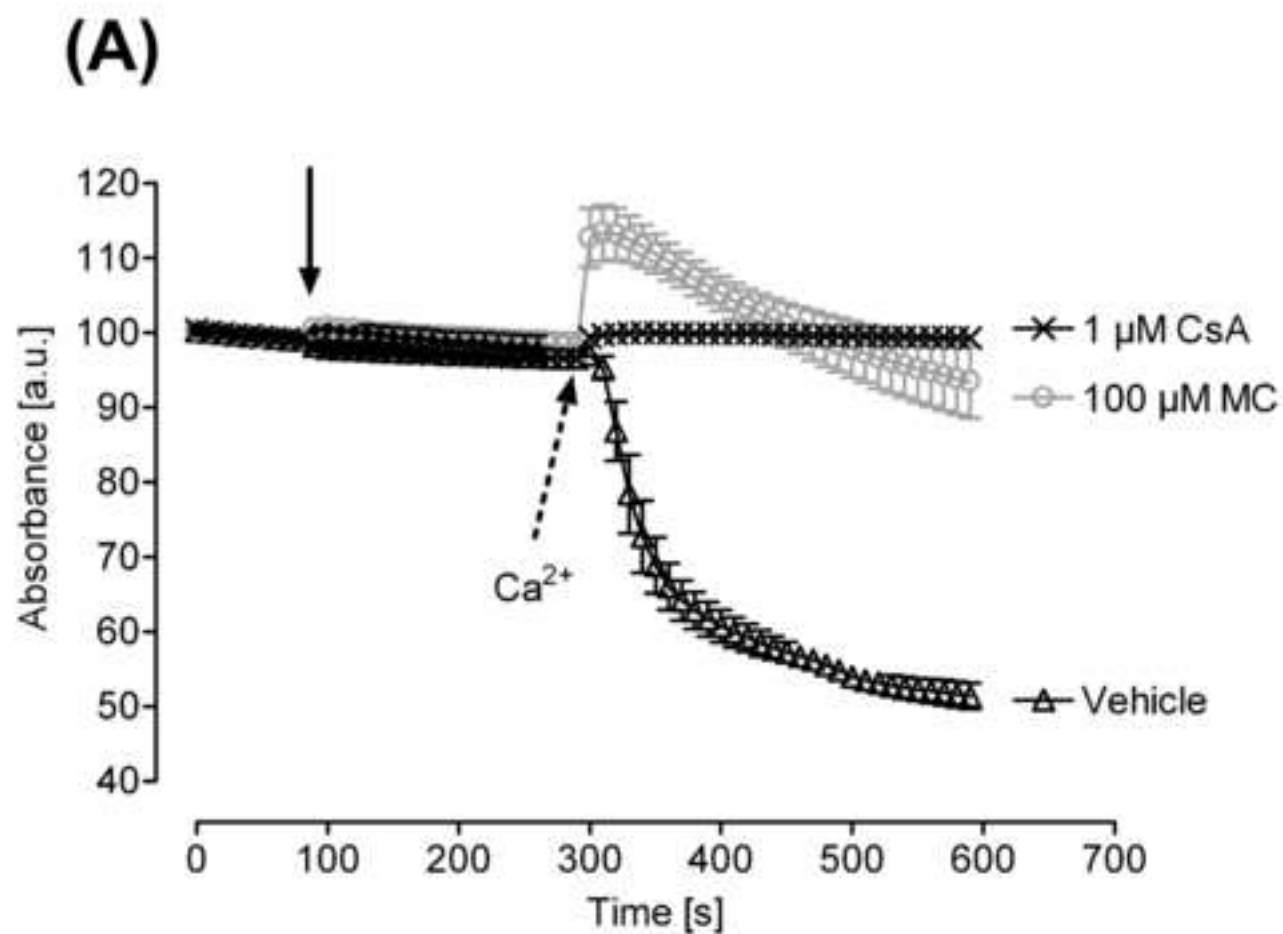


(A)

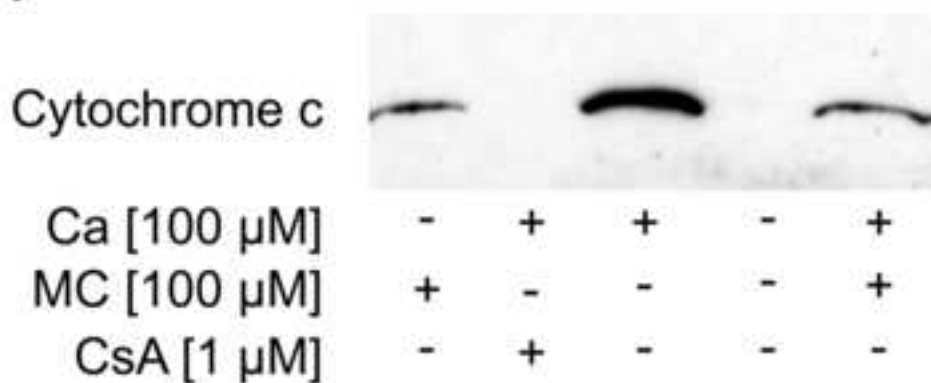


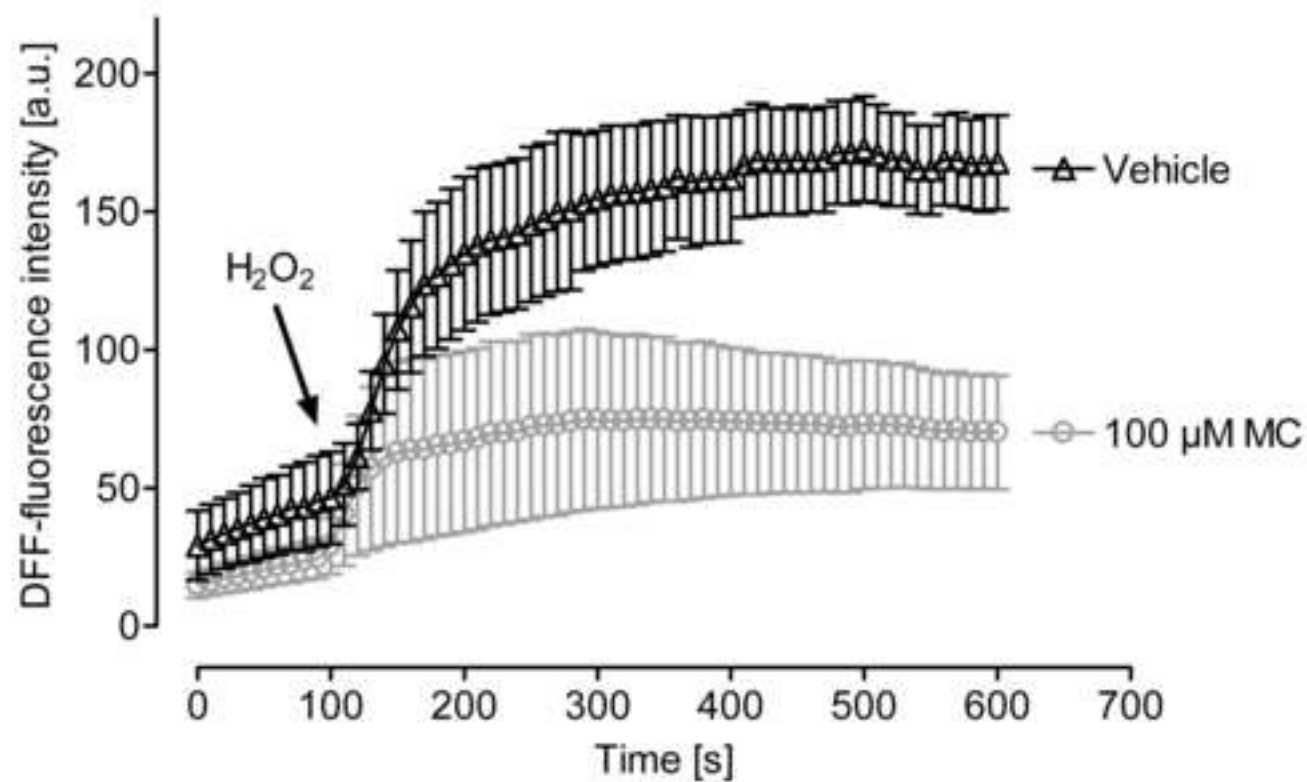
(B)





(B)



(A)**(B)**